Appendix B: Stellar population fits

Here we present examples of the stellar population modelling for each object, using the best fitting combination of metallicities presented in Table A.2. In each plot, the main panel shows the SDSS data in black with the results of the STARLIGHT modelling overlayed in red. The inset in the main panel shows a zoom of the fit around the region of the higher order Balmer absorption features characteristic of YSPs. The bottom panel shows the residuals of the fit, with zero marked with a magenta line. Regions masked out of the fit are highlighted in grey and regions given double weighting are shaded in pink. Pixels flagged in the SDSS spectra are marked with green crosses and were excluded from the fit.
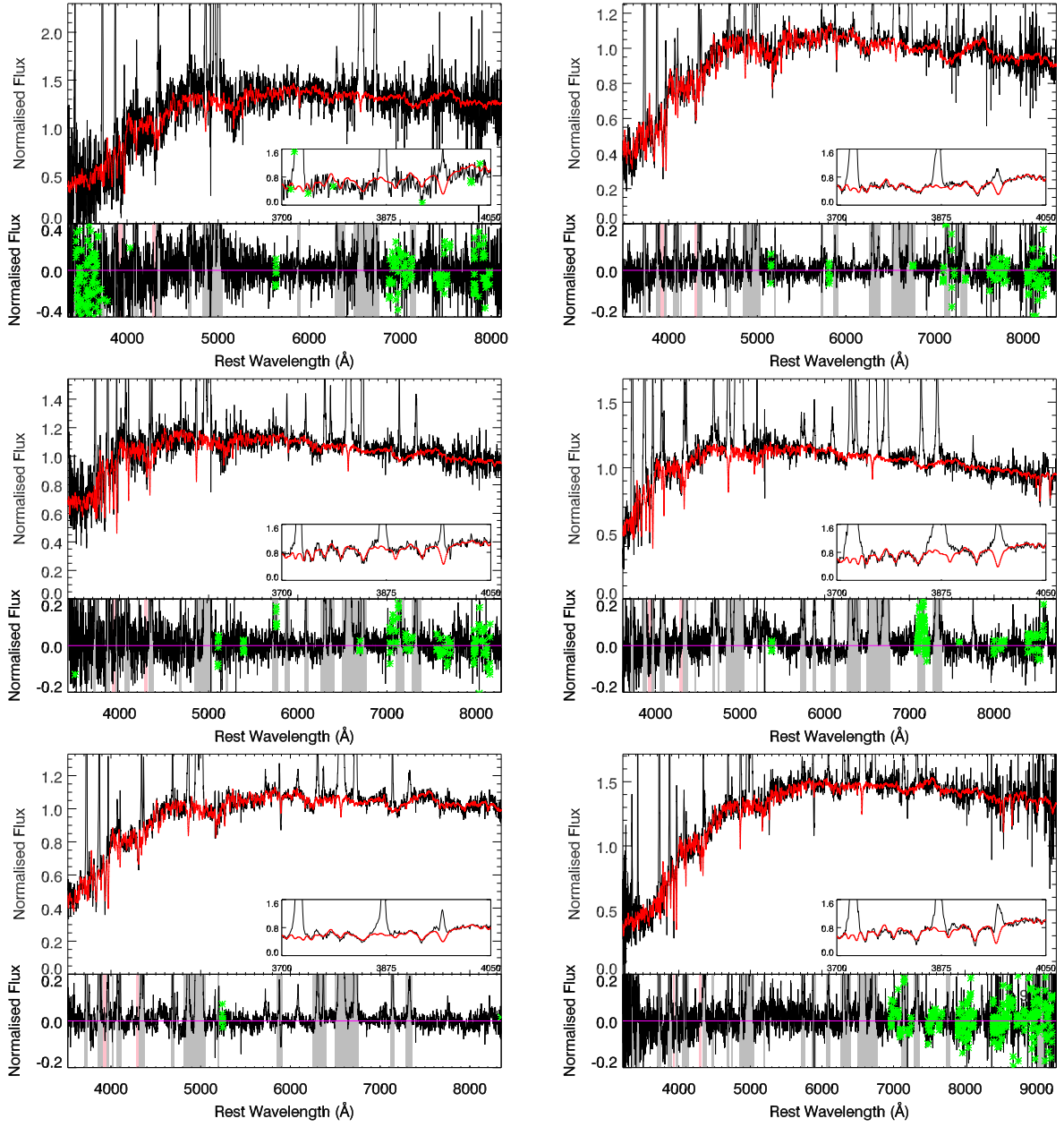
Fig. B.1: Stellar population fits of J0052-01 and J0232-08 (top row), J0731+39 and J0759+50 (middle row), and J0802+25 and J0802+46 (bottom row).
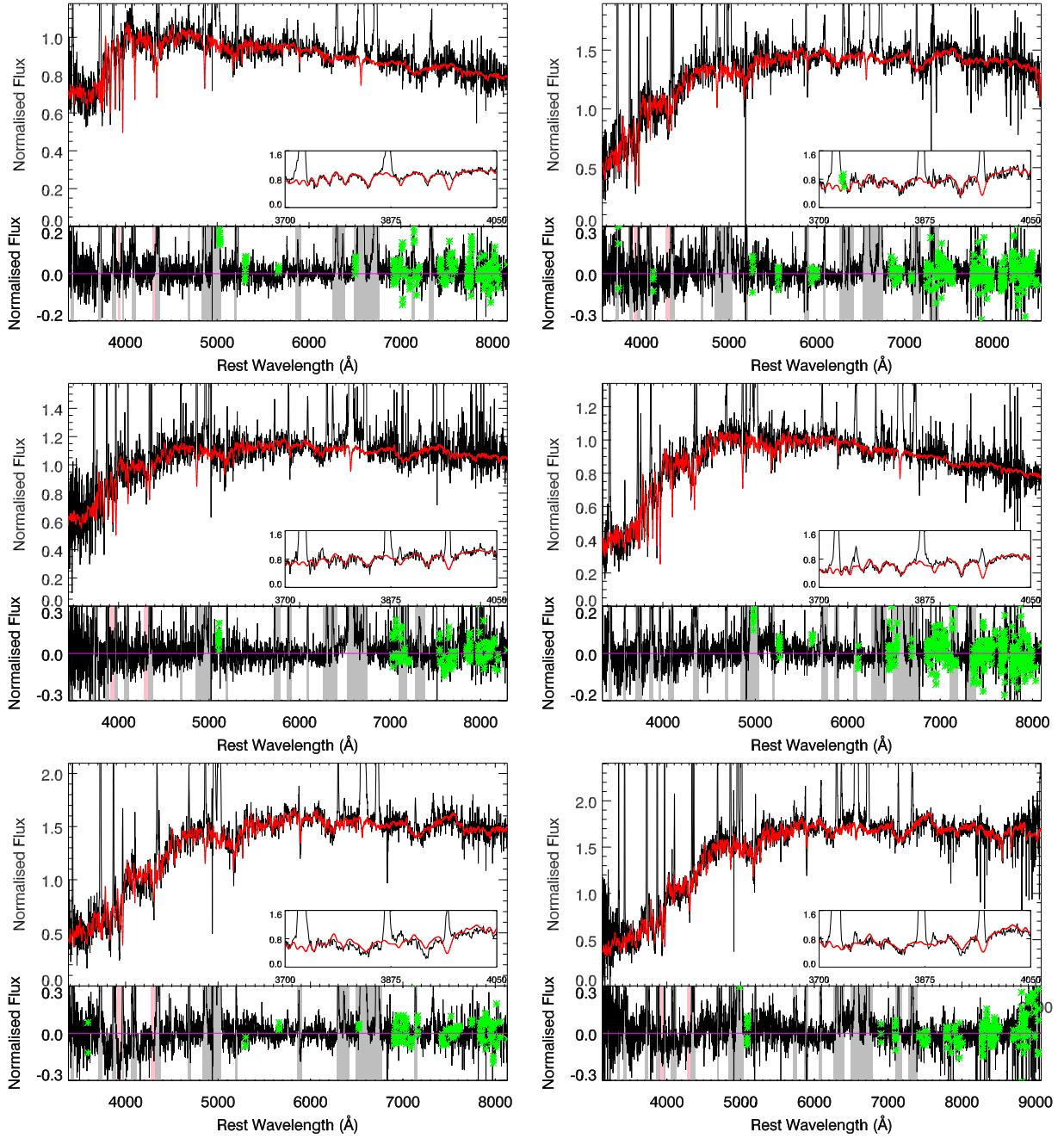
Fig. B.2: Stellar population fits of J0005+28 and J0818+36 (top row), J0841+01 and J0858+31 (middle row), and J0915+30 and J0939+35 (bottom row).
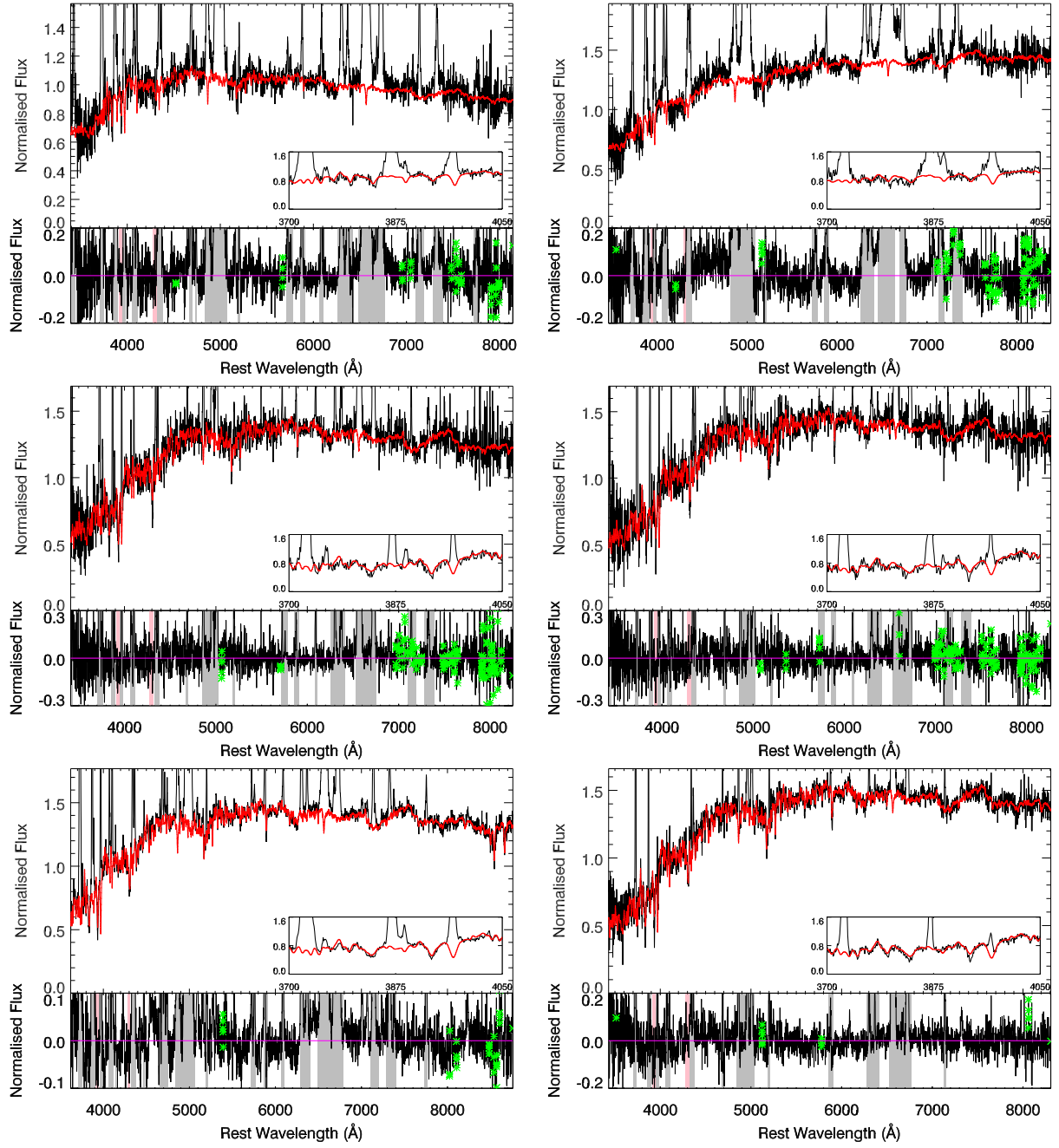
Fig. B.3: Stellar population fits of J0945+17 and J01010+06 (top row), J1015+00 and J1016+00 (middle row), and J1034+60 and J1036+01 (bottom row).
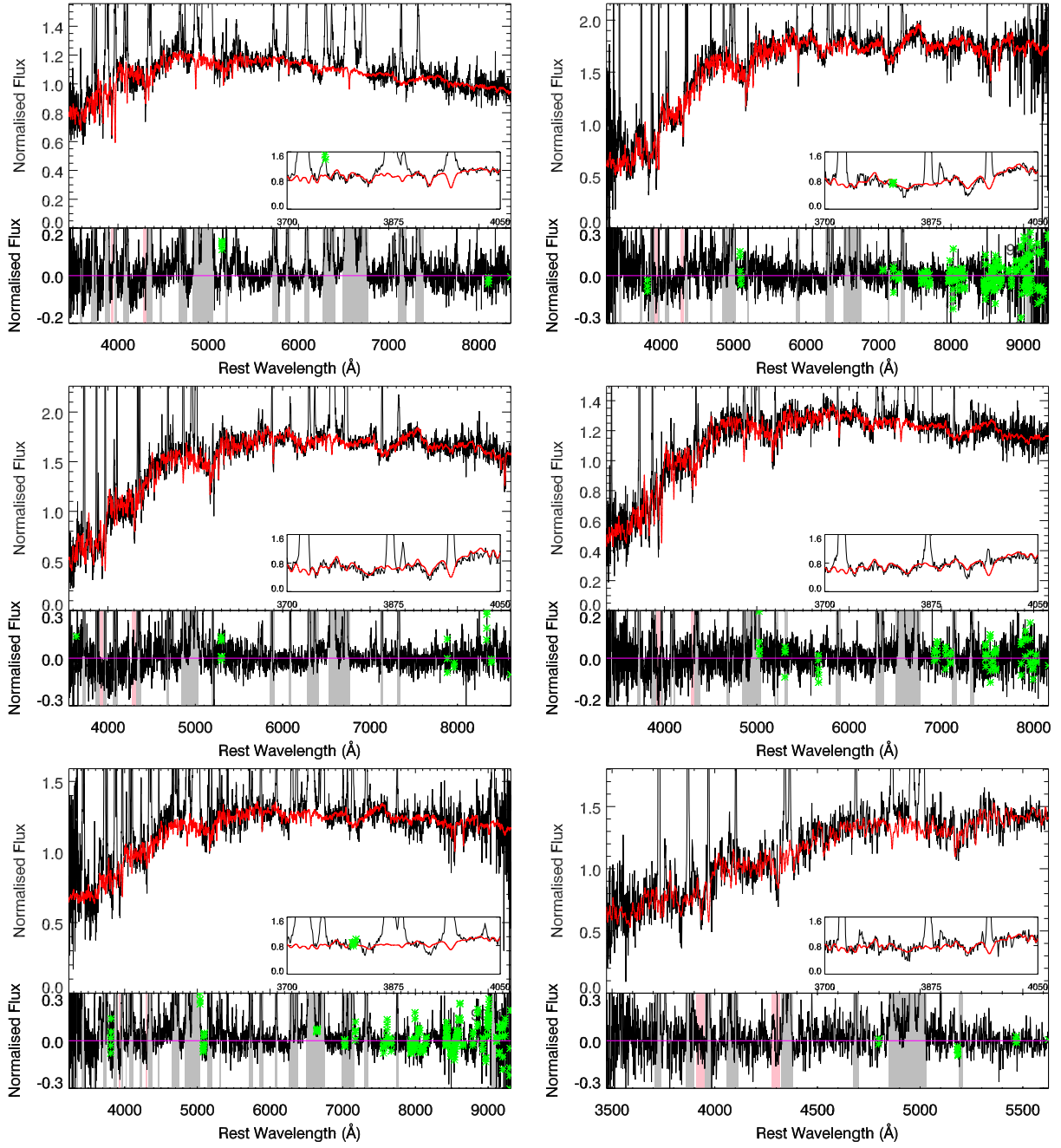
Fig. B.4: Stellar population fits of J1100+08 and J1137+61 (top row), J1152+10 and J1157+37 (middle row), and J1200+31 and J1218+47 (bottom row).
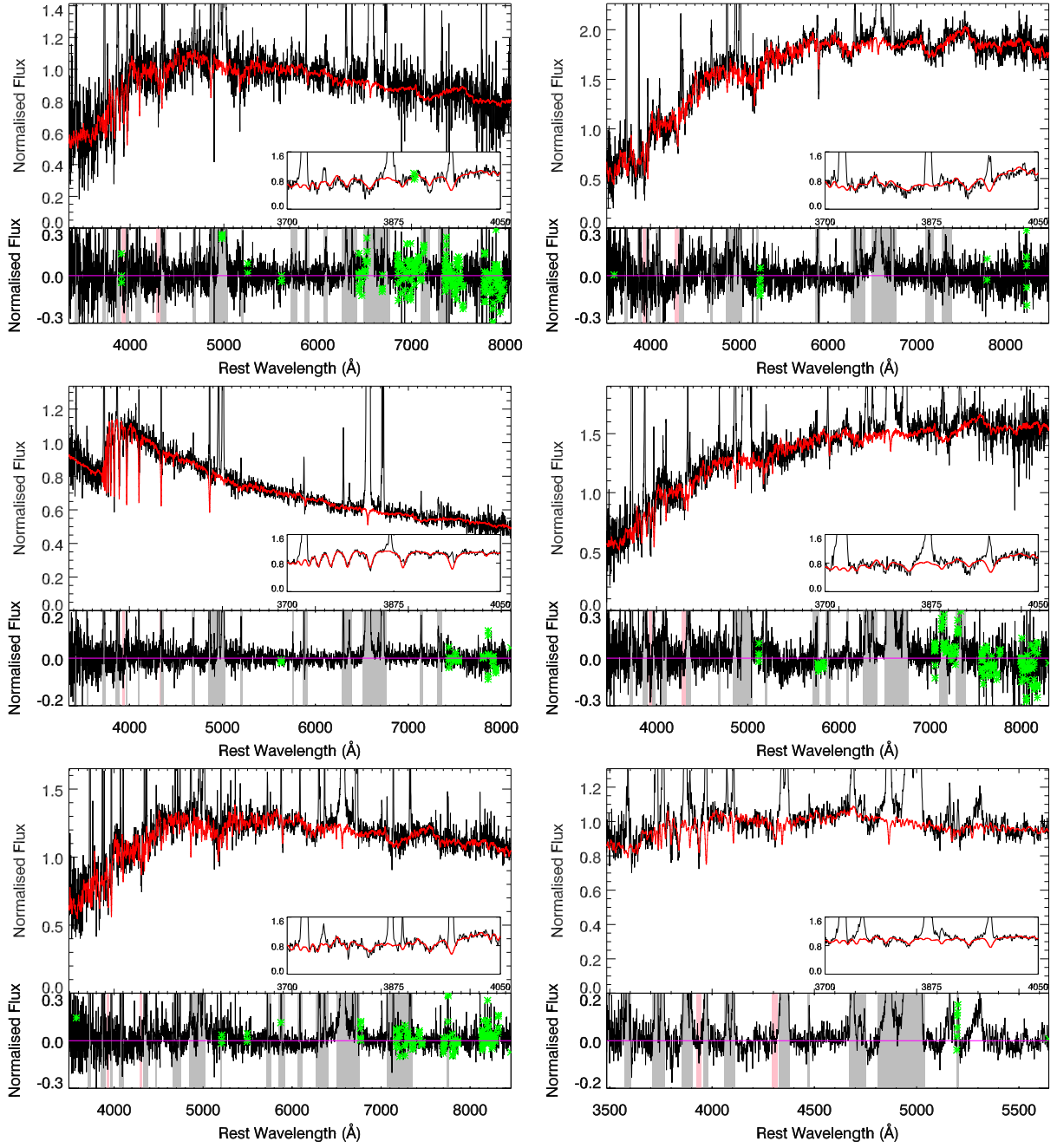
Fig. B.5: Stellar population fits of J1223+08 and J1238+09 (top row), J1241+61 and J1244+65 (middle row), and J1300+54 and J1316+44 (bottom row).

Fig. B.6: Stellar population fits of J1347+12 and J1405+40 (top row), J1356-02 and J1356+10 (middle row), and J1430+13 and J1436+13 (bottom row).
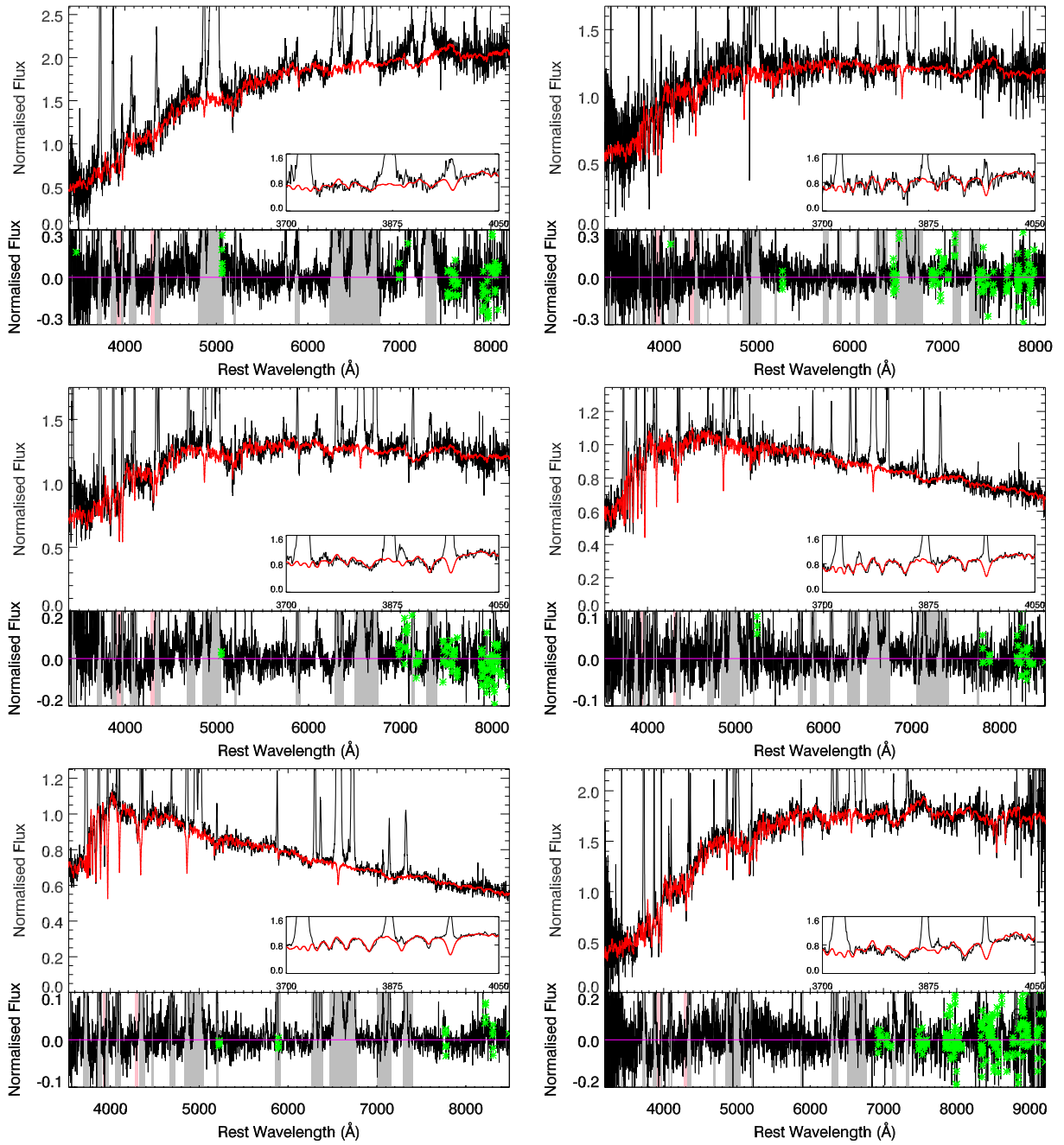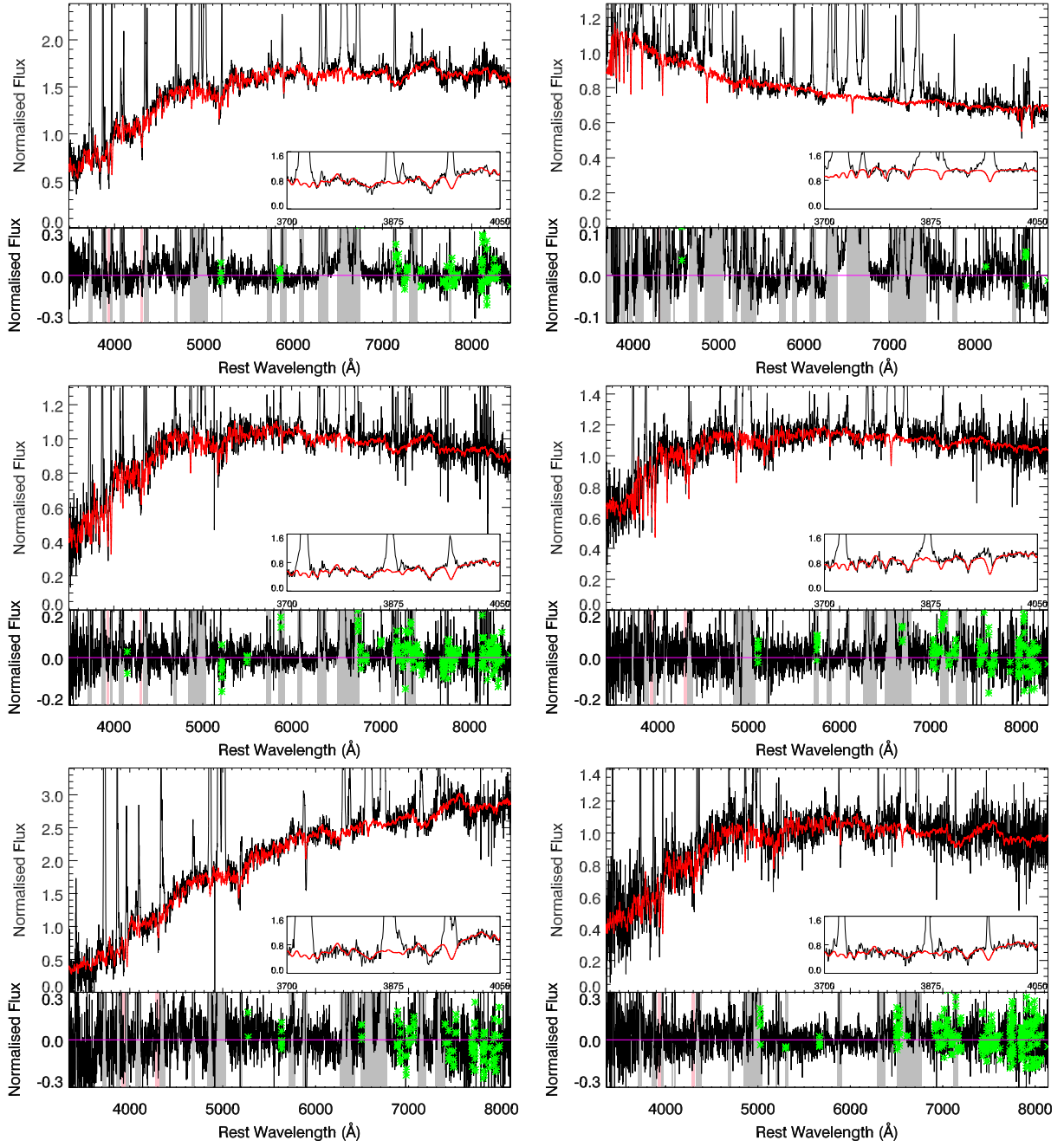
Fig. B.7: Stellar population fits of J1437+30 and J1440+53 (top row), J1455+32 and J1509+04 (middle row), and J1517+33 and J1533+35 (bottom row).
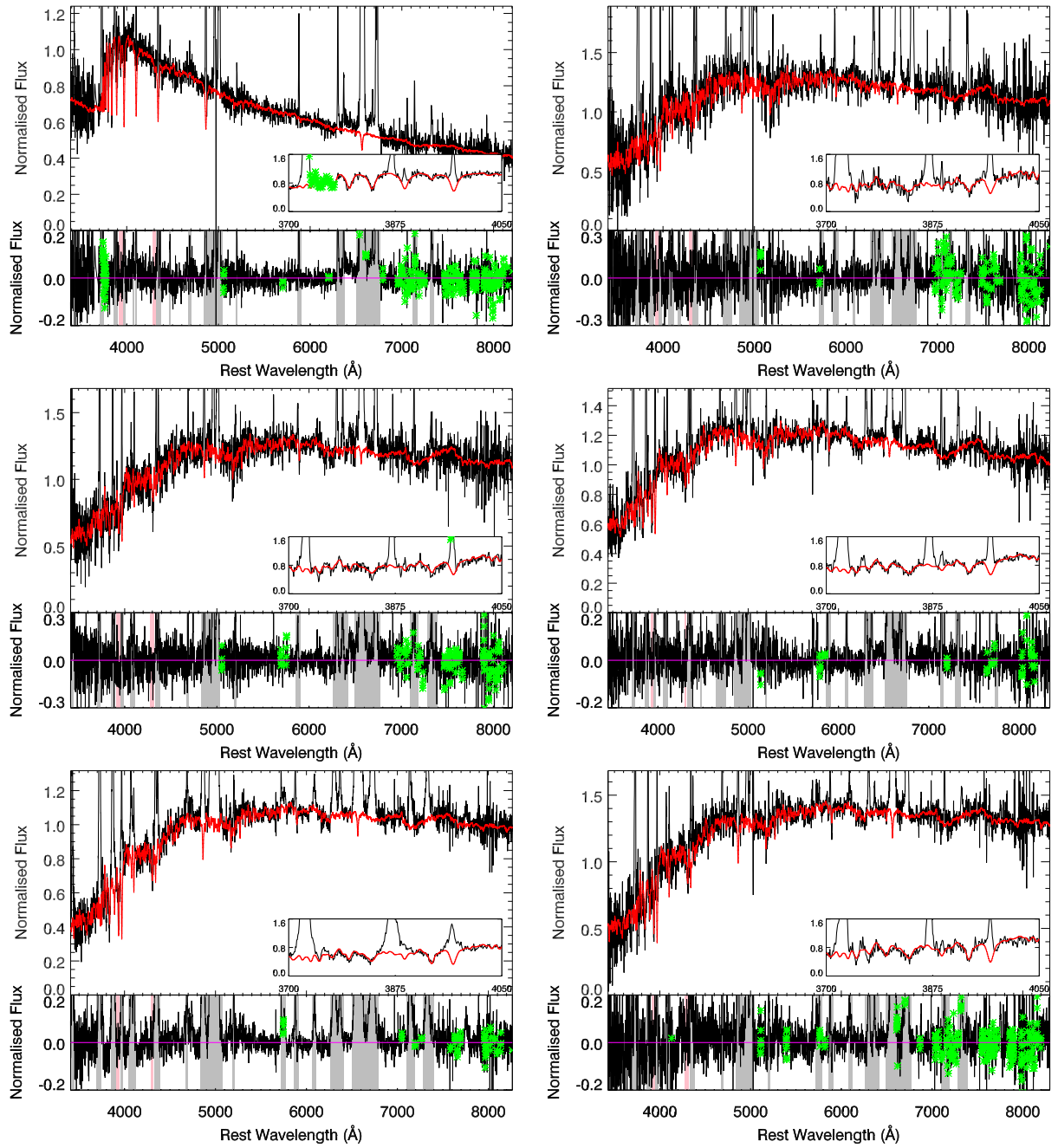
Fig. B.8: Stellar population fits of J1548-01 and J1558+35 (top row), J1624+33 and J1653+23 (middle row), and J1713+57 and J2154+11 (bottom row).

Appendix C: Emission line fitting and
 non-parametric measurements
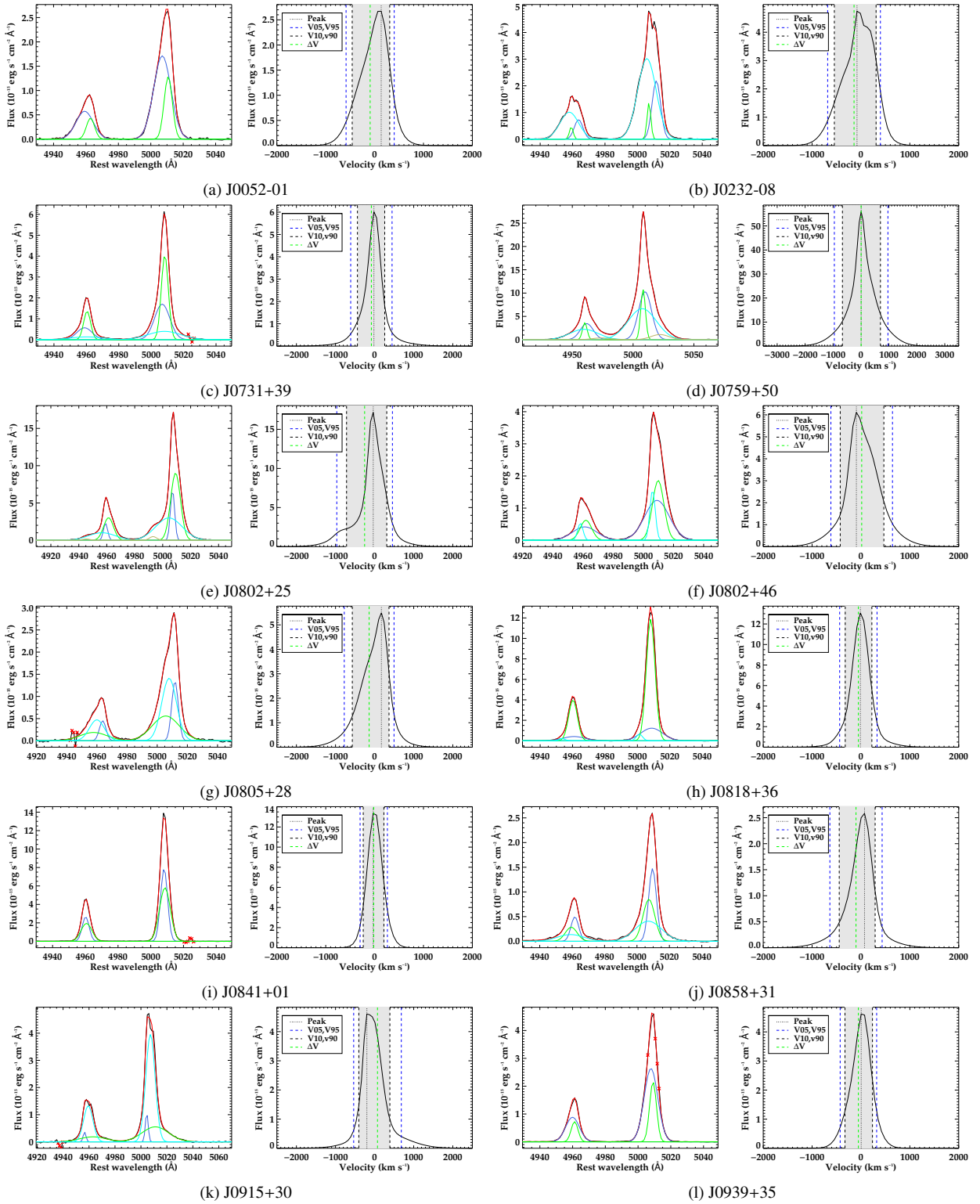
Fig. C.1: Gaussian fits to [OIII]$\lambda\lambda$4959, 5007 and non-parametric fits to [OIII]λ5007 emission lines. For each object the Gaussian fit is shown in the left panel, where he black line shows the data and and the red line shows the sum of the Gaussian components which are denoted in shades of blue and green. The red crosses show pixels that were masked out of the fit. The right panels show the corresponding non-parametric values derived from the emission line models.

(a) J0945+17

(b) J1010+06

(c) J1015+00

(d) J1016+00

(e) J1034+60

(f) J1036+01

(g) J1100+08

(h) J1137+61

(i) J1152+10

(j) J1157+37

(k) J1200+31

(l) J1218+47

Fig. C.2: Same as Figure C.1

(a) J1223+08

(b) J1238+09

(c) J1241+61

(d) J1244+65

(e) J1300+54

(f) J1316+44

(g) J1347+12

(h) J1356-02

(i) J1356+10

(j) J1405+40

(k) J1430+13

(l) J1436+13

Fig. C.3: Same as Figure C.1

(a) J1437+30

(b) J1440+53

(c) J1455+32

(d) J1509+04

(e) J1517+33

(f) J1533+35
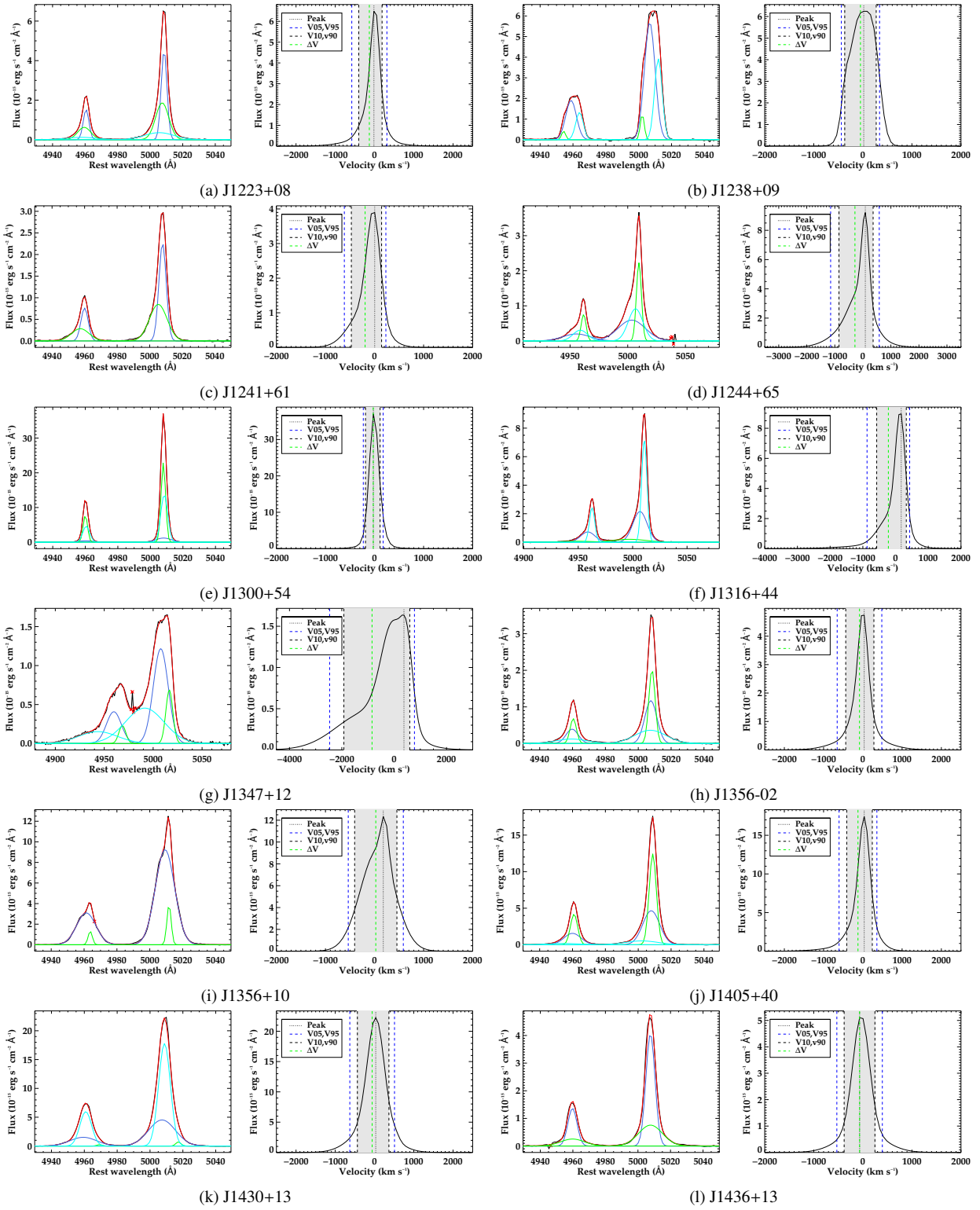
(g) J1548-01

(h) J1558+35

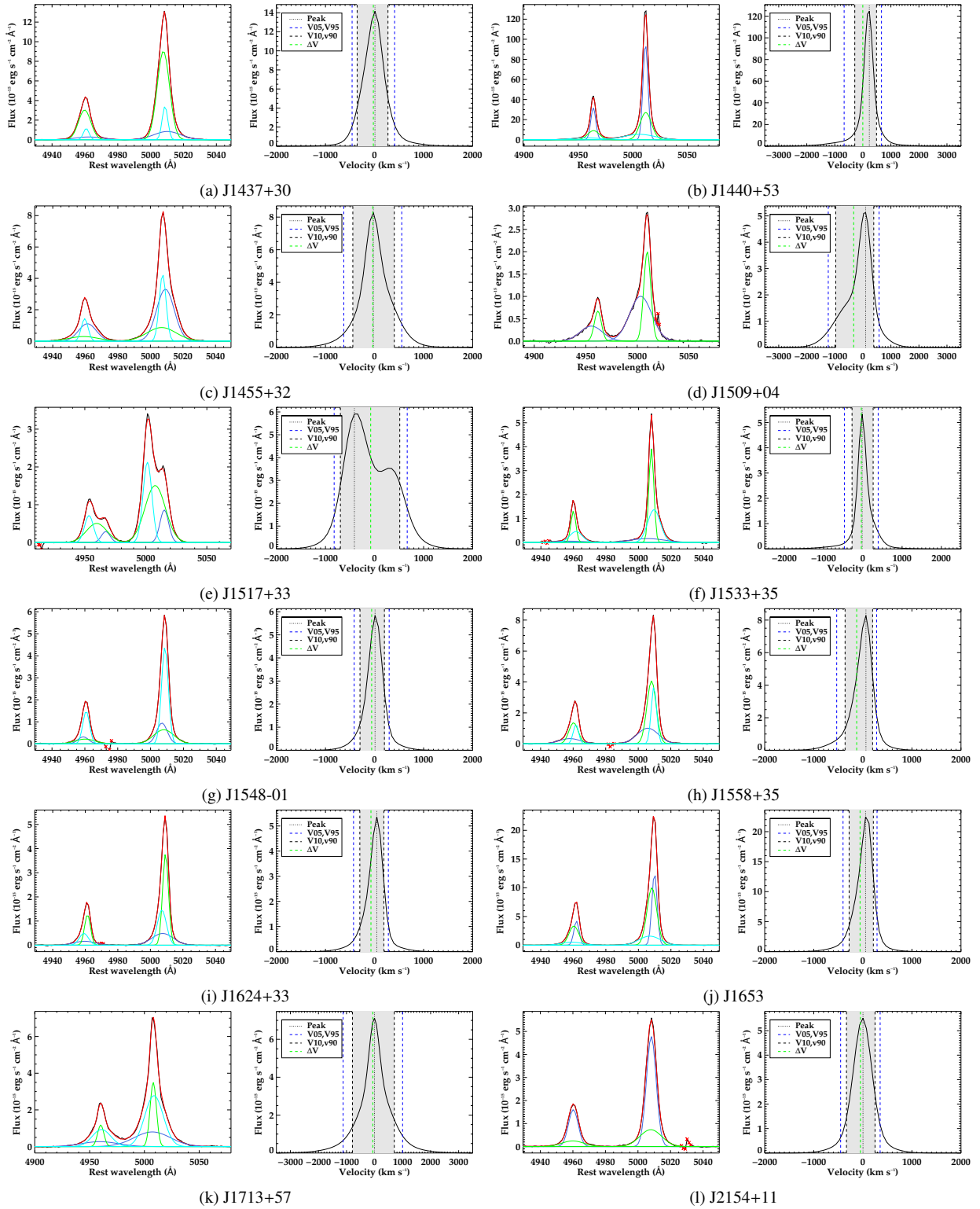(i) J1624+33

(j) J1653

(k) J1713+57
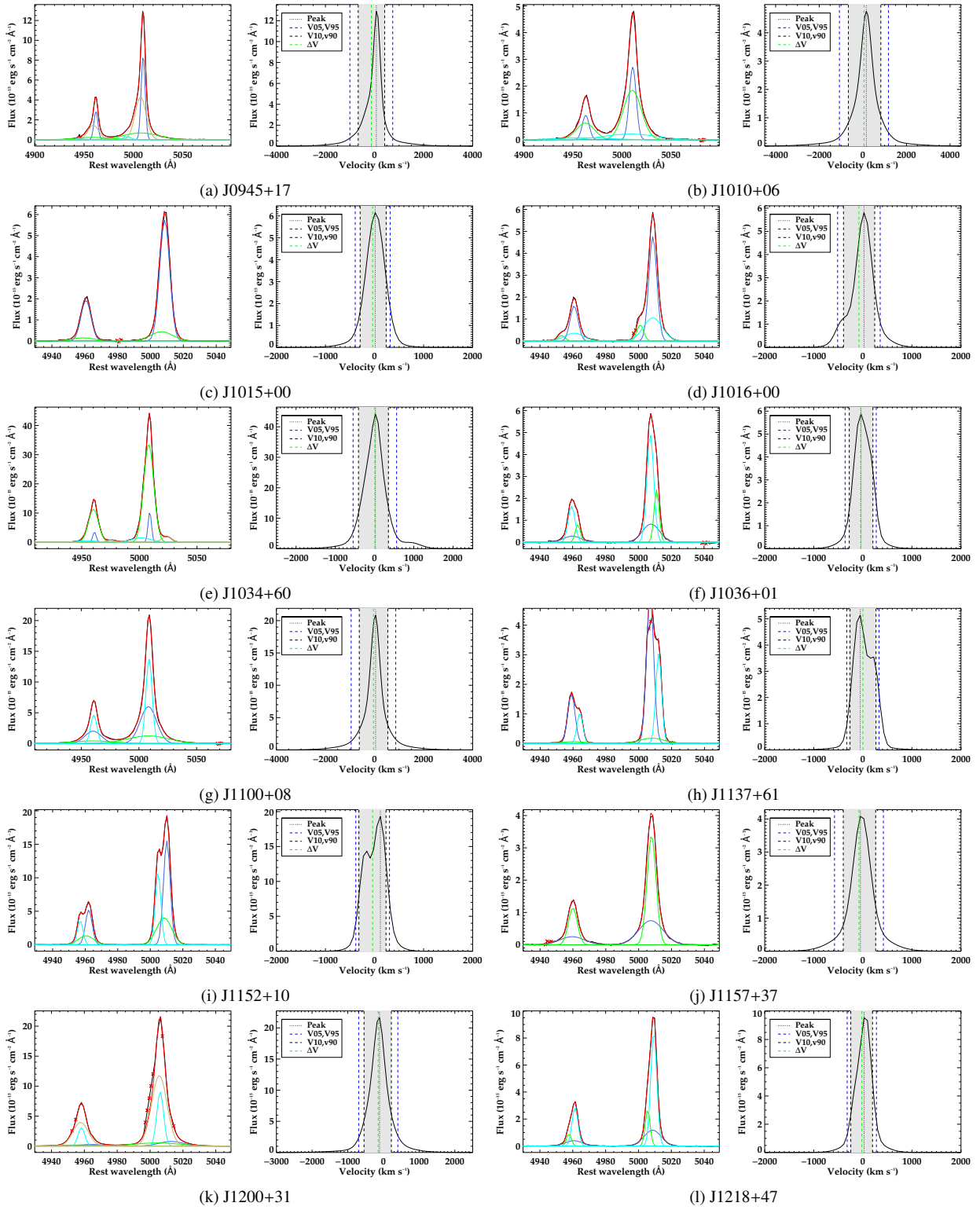
(l) J2154+11

Fig. C.4: Same as Figure C.1

Appendix D: Alternative outflow properties

Table D.1: Results of the calculations of the outflow masses, outflow mass rates, and kinetic energy rates assuming that all gas with velocities greater than 1.5 times the FWHM of the stellar velocity dispersion derived from the STARLIGHT modelling.

| Name | $\log(M_{of})$ | 0.15 kpc | | 0.62 kpc | | 1.89 kpc | |
| | | $\dot{M}_{of}$ | $\log \dot{E}_{of}$ | $\dot{M}_{of}$ | $\log \dot{E}_{of}$ | $\dot{M}_{of}$ | $\log \dot{E}_{of}$ |
	$(M_\odot)$	$(M_\odot \ yr^{-1})$	$(M_\odot \ yr^{-1})$	$(erg \ s^{-1})$	$(M_\odot \ yr^{-1})$	$(erg \ s^{-1})$	$(erg \ s^{-1})$
J0052-01	5.87 ± 0.08	5.65 ± 1.04	41.43 ± 0.10	1.36 ± 0.25	40.81 ± 0.10	0.45 ± 0.08	40.33 ± 0.10
J0232-08	5.46 ± 0.03	2.39 ± 0.20	41.14 ± 0.06	0.58 ± 0.05	40.52 ± 0.06	0.19 ± 0.02	40.04 ± 0.06
J0731+39	4.90 ± 0.04	0.51 ± 0.05	40.28 ± 0.06	0.12 ± 0.01	39.66 ± 0.06	0.041 ± 0.004	39.18 ± 0.06
J0759+50	5.23 ± 0.02	1.64 ± 0.08	41.06 ± 0.04	0.39 ± 0.02	40.45 ± 0.04	0.13 ± 0.01	39.96 ± 0.04
J0802+25	5.51 ± 0.00	3.54 ± 0.01	41.577 ± 0.002	0.851 ± 0.002	40.958 ± 0.002	0.281 ± 0.001	40.477 ± 0.002
J0802+46	5.09 ± 0.03	1.03 ± 0.09	40.76 ± 0.06	0.25 ± 0.02	40.14 ± 0.06	0.08 ± 0.01	39.66 ± 0.06
J0805+28	5.41 ± 0.01	1.99 ± 0.07	41.01 ± 0.02	0.48 ± 0.02	40.39 ± 0.02	0.16 ± 0.01	39.91 ± 0.02
J0818+36	4.86 ± 0.06	0.51 ± 0.07	40.31 ± 0.08	0.12 ± 0.02	39.69 ± 0.08	0.04 ± 0.01	39.21 ± 0.08
J0858+31	6.06 ± 0.05	7.95 ± 0.98	41.55 ± 0.07	1.91 ± 0.24	40.93 ± 0.07	0.63 ± 0.08	40.45 ± 0.07
J0915+30	5.46 ± 0.05	2.75 ± 0.36	41.27 ± 0.09	0.66 ± 0.09	40.65 ± 0.09	0.22 ± 0.03	40.17 ± 0.09
J0945+17	6.06 ± 0.05	11.39 ± 1.46	41.96 ± 0.07	2.74 ± 0.35	41.34 ± 0.07	0.90 ± 0.12	40.86 ± 0.07
J1010+06	4.46 ± 0.03	0.36 ± 0.03	40.61 ± 0.05	0.09 ± 0.01	39.99 ± 0.05	0.028 ± 0.002	39.51 ± 0.05
J1015+00	5.47 ± 0.09	1.96 ± 0.40	40.83 ± 0.09	0.47 ± 0.10	40.22 ± 0.09	0.16 ± 0.03	39.73 ± 0.09
J1016+00	5.95 ± 0.03	7.42 ± 0.50	41.61 ± 0.04	1.79 ± 0.12	41.00 ± 0.04	0.59 ± 0.04	40.51 ± 0.04
J1034+60	5.98 ± 0.02	8.27 ± 0.41	41.67 ± 0.03	1.99 ± 0.10	41.05 ± 0.03	0.66 ± 0.03	40.57 ± 0.03
J1100+08	5.58 ± 0.02	3.50 ± 0.21	41.36 ± 0.05	0.84 ± 0.05	40.74 ± 0.05	0.28 ± 0.02	40.26 ± 0.05
J1152+10	5.32 ± 0.08	1.23 ± 0.22	40.54 ± 0.08	0.30 ± 0.05	39.92 ± 0.08	0.10 ± 0.02	39.44 ± 0.08
J1157+37	4.95 ± 0.04	0.79 ± 0.09	40.69 ± 0.07	0.19 ± 0.02	40.07 ± 0.07	0.06 ± 0.01	39.59 ± 0.07
J1200+31	6.13 ± 0.03	10.64 ± 0.84	41.70 ± 0.05	2.56 ± 0.20	41.09 ± 0.05	0.84 ± 0.07	40.60 ± 0.05
J1218+47	4.93 ± 0.12	0.44 ± 0.12	39.94 ± 0.14	0.10 ± 0.03	39.32 ± 0.14	0.03 ± 0.01	38.84 ± 0.14
J1223+08	5.16 ± 0.05	1.04 ± 0.14	40.63 ± 0.09	0.25 ± 0.03	40.01 ± 0.09	0.08 ± 0.01	39.53 ± 0.09
J1238+09	5.57 ± 0.12	2.94 ± 0.88	41.17 ± 0.15	0.71 ± 0.21	40.55 ± 0.15	0.23 ± 0.07	40.07 ± 0.15
J1241+61	5.72 ± 0.04	3.46 ± 0.41	41.11 ± 0.08	0.83 ± 0.10	40.49 ± 0.08	0.27 ± 0.03	40.01 ± 0.08
J1244+65	5.63 ± 0.03	4.07 ± 0.34	41.51 ± 0.06	0.98 ± 0.08	40.89 ± 0.06	0.32 ± 0.03	40.41 ± 0.06
J1316+44	5.34 ± 0.05	1.63 ± 0.16	40.95 ± 0.05	0.39 ± 0.04	40.33 ± 0.05	0.13 ± 0.01	39.85 ± 0.05
J1347+12	4.92 ± 0.02	1.47 ± 0.07	41.63 ± 0.04	0.35 ± 0.02	41.01 ± 0.04	0.12 ± 0.01	40.53 ± 0.04
J1356-02	5.21 ± 0.04	0.96 ± 0.14	40.44 ± 0.11	0.23 ± 0.03	39.82 ± 0.11	0.08 ± 0.01	39.34 ± 0.11
J1356+10	6.20 ± 0.04	13.74 ± 1.39	41.90 ± 0.06	3.31 ± 0.34	41.28 ± 0.06	1.09 ± 0.11	40.80 ± 0.06
J1405+40	4.97 ± 0.01	0.51 ± 0.02	40.13 ± 0.02	0.122 ± 0.004	39.51 ± 0.02	0.040 ± 0.001	39.03 ± 0.02
J1430+13	5.98 ± 0.02	8.46 ± 0.47	41.71 ± 0.03	2.04 ± 0.11	41.09 ± 0.03	0.67 ± 0.04	40.61 ± 0.03
J1436+13	5.33 ± 0.04	1.66 ± 0.18	40.89 ± 0.08	0.40 ± 0.04	40.27 ± 0.08	0.13 ± 0.01	39.79 ± 0.08
J1437+30	5.48 ± 0.06	2.34 ± 0.34	41.04 ± 0.08	0.56 ± 0.08	40.43 ± 0.08	0.19 ± 0.03	39.94 ± 0.08
J1440+53	5.47 ± 0.05	2.06 ± 0.27	40.97 ± 0.07	0.50 ± 0.07	40.36 ± 0.07	0.16 ± 0.02	39.87 ± 0.07
J1455+32	5.02 ± 0.02	0.82 ± 0.04	40.59 ± 0.03	0.20 ± 0.01	39.97 ± 0.03	0.066 ± 0.003	39.49 ± 0.03
J1509+04	5.58 ± 0.03	4.11 ± 0.30	41.65 ± 0.05	0.99 ± 0.07	41.04 ± 0.05	0.33 ± 0.02	40.55 ± 0.05
J1517+33	6.29 ± 0.03	20.67 ± 1.63	42.26 ± 0.04	4.97 ± 0.39	41.64 ± 0.04	1.64 ± 0.13	41.16 ± 0.04
J1533+35	6.11 ± 0.06	8.75 ± 1.41	41.49 ± 0.09	2.11 ± 0.34	40.87 ± 0.09	0.69 ± 0.11	40.39 ± 0.09
J1558+35	5.79 ± 0.08	3.14 ± 0.59	40.83 ± 0.11	0.76 ± 0.14	40.21 ± 0.11	0.25 ± 0.05	39.73 ± 0.11
J1624+33	4.90 ± 0.08	0.51 ± 0.09	40.22 ± 0.07	0.12 ± 0.02	39.60 ± 0.07	0.04 ± 0.01	39.12 ± 0.07
J1713+57	5.34 ± 0.02	2.53 ± 0.17	41.42 ± 0.04	0.61 ± 0.04	40.80 ± 0.04	0.20 ± 0.01	40.32 ± 0.04
J2154+11	5.25 ± 0.07	1.34 ± 0.23	40.80 ± 0.10	0.32 ± 0.06	40.18 ± 0.10	0.11 ± 0.02	39.70 ± 0.10

Notes. As previously discussed, the outflow radius is unknown, so we have calculated $\dot{M}_{of}$ assuming outflow radii of 0.15, 0.62, and 1.89 kpc. Column 2 gives the total mass of the outflow whilst columns 3 to 8 show $\dot{M}_{of}$ and $\log \dot{E}_{of}$ for each assumed radius. Only objects which have an outflow according to our definition are included in the table.